

UC San Diego

UC San Diego Previously Published Works

Title

Quantitative assessment of articular cartilage degeneration using 3D ultrashort echo time cones adiabatic T1 ρ (3D UTE-Cones-AdiabT1 ρ) imaging.

Permalink

<https://escholarship.org/uc/item/5hw4x6wh>

Journal

European Radiology, 32(9)

Authors

Wu, Mei
Ma, Ya-Jun
Liu, Mouyuan
et al.

Publication Date

2022-09-01

DOI

10.1007/s00330-022-08722-6

Peer reviewed



Published in final edited form as:

Eur Radiol. 2022 September ; 32(9): 6178–6186. doi:10.1007/s00330-022-08722-6.

Quantitative Assessment of Articular Cartilage Degeneration Using 3D Ultrashort Echo Time Cones Adiabatic $T_{1\rho}$ (3D UTE-Cones-Adiab $T_{1\rho}$) Imaging

Mei Wu^{1,2}, Ya-Jun Ma², Mouyuan Liu³, Yanping Xue², Lillian Gong², Zhao Wei², Saeed Jerban², Hyungseok Jang², Douglas G Chang⁴, Eric Y Chang^{2,5}, Liheng Ma³, Jiang Du²

¹Department of Radiology, Guangzhou First People's Hospital, School of Medicine, South China University of Technology, Guangzhou, Guangdong, China

²Department of Radiology, University of California San Diego, San Diego, 9452 Medical Center Dr., San Diego, CA 92037, USA

³Imaging Department, The First Affiliated Hospital of Guangdong Pharmaceutical University, Guangzhou, Guangdong, China

⁴Department of Orthopaedic Surgery, University of California San Diego, San Diego, CA, USA

⁵Radiology Service, Veterans Affairs San Diego Healthcare System, San Diego, CA, US

Abstract

Objectives—To evaluate articular cartilage degeneration using quantitative three-dimensional ultrashort-echo-time Cones Adiabatic- $T_{1\rho}$ (3D UTE-Cones-Adiab $T_{1\rho}$) imaging.

Methods—66 human subjects were recruited for this study. Kellgren-Lawrence (KL) grade and Whole-Organ Magnetic-Resonance-Imaging Score (WORMS) were evaluated by two musculoskeletal radiologists. The human subjects were categorized into three groups, including normal controls (KL0), doubtful-minimal osteoarthritis (OA) (KL1–2), and moderate-severe OA (KL3–4). WORMS were regrouped to encompass the extent of lesions and the depth of lesions. The UTE-Cones-Adiab $T_{1\rho}$ values were obtained using 3D UTE-Cones data acquisitions preceded by seven paired adiabatic full passage pulses that corresponded to seven spin-locking times (TSLs) of 0, 12, 24, 36, 48, 72, and 96 ms. The performance of the UTE-Cones-Adiab $T_{1\rho}$ technique in evaluating the degeneration of knee cartilage was assessed via the ANOVA comparisons with subregional analysis and Spearman's correlation coefficient as well as the receiver-operating-characteristic (ROC) curve.

Results—UTE-Cones-Adiab $T_{1\rho}$ showed significant positive correlations with KL grade ($r=0.15$, $P<0.05$) and WORMS ($r=0.57$, $P<0.05$). Higher UTE-Cones-Adiab $T_{1\rho}$ values were observed in both larger and deeper lesions in the cartilage. The differences in UTE-Cones-Adiab $T_{1\rho}$ values among different extent and depth groups of cartilage lesions were all statistically significant ($P<0.05$). Subregional analyses showed that the correlations between UTE-Cones-Adiab $T_{1\rho}$ and

WORMS varied with the location of cartilage. The AUC values of UTE-Cones-AdiabT_{1ρ} for mild cartilage degeneration (WORMS=1) was 0.8. The diagnostic threshold value of UTE-Cones-AdiabT_{1ρ} for mild cartilage degeneration was 39.4 ms with 80.8% sensitivity.

Conclusions—The 3D UTE-Cones-AdiabT_{1ρ} sequence may significantly improve the robustness of quantitative evaluation of articular cartilage degeneration.

Keywords

ultrashort echo time; AdiabT_{1ρ}; articular cartilage; degeneration; quantitative assessment

Introduction

Osteoarthritis (OA) ranks second only to cardiovascular disease as the cause of work-related disability. Therefore, it is essential to develop techniques that will improve the detection of OA at an early stage in order to facilitate more timely intervention. The loss of proteoglycans (PGs) in articular cartilage is one of the most significant early changes observed in OA. Spin lattice relaxation in the rotating frame (T_{1ρ}) has been proposed as a method to investigate the slow-motion interactions between macromolecules and water (1–4). Several in vitro studies demonstrated a highly linear relationship between T_{1ρ} relaxation and PG content (2–4), while some other studies demonstrated a weaker correlation especially in the superficial layers of articular cartilage (5). A number of in vivo studies showed elevated T_{1ρ} values in OA patients when compared to corresponding healthy subjects (6–10).

While T_{1ρ} is a promising biomarker for the detection of early OA, a major confounding factor is the magic angle effect (11). T_{1ρ} can increase by up to 100% when the collagen fibers are reoriented from 0° to near 55° relative to the B₀ field (11–15). Given that early OA can increase T_{1ρ} by only 10–30% (16), this is a major limitation in the biomarker's usefulness. Meanwhile, OA is recognized as a whole-organ disease (17–19): the failure of any involved tissue has the potential to affect the surrounding tissue, thereby contributing to failure of the joint as a whole. It is then essential that all major components in the joint are imaged for truly comprehensive assessment of OA. Unfortunately, clinical sequences are only able to assess tissues which have relatively long T₂ values, such as the more superficial layers of articular cartilage. Many joint tissues, including the deeper layers of cartilage, menisci, ligaments, tendons, and bone have short T₂ values and therefore show little to no signal when imaged with conventional clinical sequences (20).

Recent studies have shown that Adiabatic T_{1ρ} (AdiabT_{1ρ}) is sensitive to both ex vivo cartilage degradation induced by enzymatic treatment and in vivo cartilage degradation in OA patients (21–26). Furthermore, AdiabT_{1ρ} is much less sensitive to the magic angle effect than conventional T_{1ρ} and T₂ (27). The three-dimensional ultrashort echo time Cones (3D UTE-Cones) sequence allows fast volumetric imaging of both short and long T₂ tissues in the knee joint (28–29). The combination of this 3D UTE-Cones sequence with AdiabT_{1ρ} preparation (3D UTE-Cones-AdiabT_{1ρ}) allows for magic angle-insensitive imaging of various knee joint tissues (30–32), but the clinical performance of such a combination in evaluating cartilage degeneration remains unknown.

This study aimed to further evaluate the feasibility and efficacy of 3D UTE-Cones-AdiabT_{1ρ} imaging for in vivo assessment of whole knee cartilage in healthy volunteers and patients with varying degrees of OA. The relationship between the subregional and global UTE-Cones-AdiabT_{1ρ} values of articular cartilage and clinical evaluation of OA patients measured by Kellgren-Lawrence (KL) grade and Whole-Organ Magnetic Resonance Imaging Score (WORMS) were investigated (10,33).

Methods

Subjects

This study was approved by the local Institutional Review Board (IRB). A total of 66 human subjects (aged 23–88 years, mean age of 54±16 years, 32 females, 34 males), including 20 asymptomatic healthy volunteers and 46 patients with different degrees of OA, were recruited from July 2017 to July 2019. Written informed consent was obtained from each subject in accordance with the IRB guidelines. Asymptomatic volunteers had no history of diagnosed OA, no knee pain, and no functional impairment or moderate to severe physical symptoms in the past six months in either knee joint. The criteria for OA patients were based on KL grades obtained from plain radiographs. Exclusion criteria included a history of surgery, an inability to complete the MRI scan, and a WORMS of 6 (i.e., diffuse (75% of the region) full-thickness cartilage loss).

Data acquisition

The whole knee joint (27 left knees, 39 right knees) was scanned using the 3D UTE-Cones-AdiabT_{1ρ} sequence on a 3T MR750 scanner (GE Healthcare Technologies, Milwaukee, WI). An 8-channel knee coil was used for signal excitation and reception. The sequence employed unique k-space trajectories that sampled data along evenly spaced twisting paths in the shape of multiple cones (34) and the 3D UTE data acquisition started as soon as possible following a short rectangular radiofrequency (RF) pulse excitation with a minimal nominal echo time (TE) of 32 μs. T_{1ρ} contrast was generated using identical non-selective adiabatic inversion recovery (IR) pulses (adiabatic full passage hyperbolic secant type 1 pulse) with a duration of 6.048 ms, bandwidth of 1.643 kHz, and maximum B₁ amplitude of 17 μT (30). The adiabatic IR pulses allow uniform inversion of longitudinal magnetizations when the adiabatic condition is satisfied, making them insensitive to B₁ inhomogeneities (35). An even number of adiabatic IR pulses (N_{IR}) was used to keep the longitudinal magnetizations positive for AdiabT_{1ρ} preparation and a spoiling gradient was used to crush the remaining transverse magnetizations following the train of AdiabT_{1ρ} pulses. Multiple spiral spokes (N_{sp}) were acquired after each AdiabT_{1ρ} preparation to speed up data acquisition.

Imaging parameters for the 3D UTE-Cones-AdiabT_{1ρ} sequence included the following: repetition time (TR) = 500 ms; flip angle (FA) = 10°; acquisition matrix = 256×256×36, N_{sp} = 25; N_{IR} = 0, 2, 4, 6, 8, 12, and 16, corresponding to spin-locking times (TSLs) of 0, 12, 24, 36, 48, 72, and 96 ms, respectively; scan time of 2 min 34 sec for each set of UTE-Cones-AdiabT_{1ρ} data. Following the AdiabT_{1ρ} preparation, a conventional chemical shift-based fat saturation pulse was used to suppress signal from marrow fat. Because a 500

ms TR is relatively short, T1 compensation was needed for accurate AdiabT_{1ρ} mapping. T1 mapping was achieved using a UTE variable flip angle (UTE-VFA) sequence with TR = 20 ms, FA = 5°, 10°, 20°, and 30°, matrix = 256×256×36, and a total scan time = 9 min 28 sec (36). For correction of T1 and AdiabT_{1ρ} measurements, B1 mapping was achieved using 3D UTE-Cones actual flip angle imaging (AFI) with TR₁/TR₂ = 20/100 ms, FA = 45°, matrix = 128×128×18, and a total scan time = 4 min 57 sec (37). Radiography and sagittal fat-suppressed T2-weighted FSE and PD-weighted images were also obtained for KL grade and WORMS (33).

Data analysis

To compensate for motion between the different 3D UTE-Cones datasets, elastix-based motion registration was applied to all quantitative 3D UTE-Cones-AdiabT_{1ρ} and T₁ mapping images, where a rigid affine transform was followed by a non-rigid b-spline registration (38). UTE-Cones-AdiabT_{1ρ} of whole knee articular cartilage was quantified using a single-component exponential fitting model as previously described (30). T₁ mapping was applied using non-linear optimization based on a Levenberg-Marquardt algorithm (36) and all analysis of acquired UTE images was performed using MATLAB 2017b (The MathWorks, Natick, MA, USA) code that was developed in-house.

Each whole knee was independently scored by two experienced musculoskeletal radiologists (M.W. and Y.X.) with 23 and 19 years of experience, respectively, according to KL grade and WORMS. Then, all subjects were classified into three groups according to KL grade: normal controls (KL= 0), doubtful-minimal OA (KL 2), and moderate-severe OA (KL 3) (8,10). The whole knee articular cartilage was next divided into 13 subregions (Figure 1) and the two radiologists individually drew ROIs onto images of each subregion. These subregions were then scored slice-by-slice according to WORMS and classified into seven groups: WORMS = 0, 1, 2, 2.5, 3, 4, and 5. Subregion cartilages were further divided into two respective subcategories according to the extent and depth of cartilage lesions (10,33). The extent groups included WORMS 0 (controls); WORMS 1, 2, and 2.5 (regional lesions); and WORMS 3, 4, and 5 (diffuse lesions). The depth groups included WORMS 0 (controls); WORMS 1, 2, 3, and 4 (partial thickness lesions); and WORMS 2.5 and 5 (full-thickness lesions) (10,39). The DICOM images were analyzed using MATLAB 2017b and respective correlations between 3D UTE-Cones-AdiabT_{1ρ} values and both KL grade and WORMS were analyzed.

Statistical Analysis

Intraclass correlation efficient (ICC) was used to evaluate consistency between the two radiologists. The correlations between UTE-Cones-AdiabT_{1ρ} and both KL grade and WORMS (all WORMS scores and by WORMS categories) were evaluated using Spearman's correlation coefficient. The differences in UTE-Cones-AdiabT_{1ρ} among different groups based on KL grade and WORMS were assessed and compared using one-way analysis of variance (ANOVA) after normality test. When a significant difference existed, Tukey-Kramer test was used for post-hoc multiple comparisons. Receiver operating characteristic (ROC) and area under the curve (AUC) were used to evaluate the diagnostic efficacy of UTE-Cones-AdiabT_{1ρ} for the detection of doubtful-minimal OA (KL=1–2)

and mild cartilage degeneration (WORMS=1). P-values of less than 0.05 were considered statistically significant. All statistical analyses were performed using SPSS (IBM, Armonk, NY, USA) version 25.0.

Results

A total of 713 cartilage subregions from 66 human subjects were analyzed, including 3D UTE-Cones-AdiabT_{1ρ} data selected from 3,707 slices. Excellent inter-observer agreement (ICC=0.938–0.966, P<0.05) was achieved between the two radiologists for KL grading, WORMS grading, and quantitative analyses. The groupings of subjects and cartilage subregions are shown in Table 1.

Figure 2 shows representative UTE-Cones-AdiabT_{1ρ} fitting in the anterior subregions of femoral cartilage of two human subjects, including a healthy volunteer (36 years old) and a patient with doubtful-minimal OA (43 years old). Excellent single-component exponential fitting was achieved for both ROIs drawn in the anterior subregions of femoral cartilage, demonstrating UTE-Cones-AdiabT_{1ρ} values of 35.8±5.3 ms and 42.8±5.7 ms, respectively. Similar exponential fitting was achieved for all the UTE-Cones-AdiabT_{1ρ} data. Figure 3 shows the boxplot of UTE-Cones-AdiabT_{1ρ} values in different WORMS groups. Statistically significant differences were observed in UTE-Cones-AdiabT_{1ρ} values between WORMS extent groups and depth groups.

The mean UTE-Cones-AdiabT_{1ρ} values of cartilage were 37.3±5.45 ms for normal controls, 39.1±6.46 ms for doubtful-minimal OA, and 39.0±6.42 ms for moderate-severe OA. Table 2 shows the values of UTE-Cones-AdiabT_{1ρ} in different WORMS groups. Higher UTE-Cones-AdiabT_{1ρ} values were observed in both larger and deeper lesions, with 44.1±5.6 ms for cartilage with diffuse lesions and 46.8±6.5 ms for cartilage with full-thickness lesions compared to 35.5±4.9 ms for normal cartilage.

The Spearman's correlation coefficient showed a positive relationship between the UTE-Cones-AdiabT_{1ρ} values and the corresponding KL grades (r=0.15, P<0.05) and WORMS (r=0.57, P<0.05). Results showed a similar positive relationship between UTE-Cones-AdiabT_{1ρ} and different extent groups (r =0.57, P<0.05) and depth groups (r =0.57, P<0.05). Subregional analyses showed that the correlation between UTE-Cones-AdiabT_{1ρ} and WORMS varied with the location of cartilage. Stronger correlations (r=0.61 to 0.75, P<0.05) of UTE-Cones-AdiabT_{1ρ} with WORMS were observed in the central subregions of medial femoral cartilage, the posterior subregions of lateral femoral cartilage, and the anterior subregions of medial tibial cartilage, but lower correlations (r=0.28 to 0.39, P<0.05) were found in other subregions such as the posterior subregions of lateral tibial cartilage, as shown in Table 3.

Differences in the UTE-Cones-AdiabT_{1ρ} values among KL groups (i.e., controls vs. doubtful-minimal OA, controls vs. moderate-severe OA) were statistically significant (P<0.05), but the difference between doubtful-minimal OA and moderate-severe OA was not significant. The UTE-Cones-AdiabT_{1ρ} values were significantly different among WORMS groups (i.e., WORMS=0 vs. different degree lesions groups, WORMS=1 vs. WORMS=2.5,

WORMS=1 vs. WORMS=5, WORMS=2 vs. WORMS=5, WORMS=3 vs. WORMS=5) ($P<0.05$), but there was no significant difference among other different lesion groups. UTE-Cones-AdiabT_{1ρ} differences among different extent groups of cartilage lesions (i.e., controls vs. regional lesions, controls vs. diffuse lesions, regional lesions vs. diffuse lesions) were statistically significant ($P<0.05$). For different depth groups, the difference between controls vs. partial thickness lesions, controls vs. full-thickness lesions, and partial thickness lesions vs. full-thickness lesions were all statistically significant ($P<0.05$).

Figure 4 shows the ROC curves which suggest that UTE-Cones-AdiabT_{1ρ} could distinguish doubtful-minimal OA (KL=1–2) from normal controls (KL=0), and mild cartilage degeneration (WORMS=1) from normal cartilage (WORMS 0). The AUC values of UTE-Cones-AdiabT_{1ρ} were 0.6 (95% confidence interval (CI): 0.6–0.7) for doubtful-minimal OA (KL=1–2) and 0.8 (95% CI: 0.7–0.8) for mild cartilage degeneration (WORMS=1). The diagnostic threshold value of UTE-Cones-AdiabT_{1ρ} for doubtful-minimal OA was 38.5 ms with 64.5% sensitivity and 54.5% specificity, and the diagnostic threshold value of UTE-Cones-AdiabT_{1ρ} for mild cartilage degeneration was 39.4 ms with higher sensitivity (80.8%) and specificity (63.5%).

Discussion

In this study, we evaluated whole knee full-thickness cartilage using 3D UTE-Cones-AdiabT_{1ρ} on a clinical 3T scanner and investigated its clinical application in different stages of OA in vivo. The UTE-Cones-AdiabT_{1ρ} value showed a significant positive correlation with both KL grade and WORMS and demonstrated promising value in the detection of cartilage degeneration. The technique was able to distinguish mild cartilage degeneration (WORMS 1) from normal cartilage (WORMS 0), with greater increases in UTE-Cones-AdiabT_{1ρ} values for the central subregions of medial femoral cartilage, the posterior subregions of lateral femoral cartilage, and the anterior subregions of medial tibial cartilage. A higher UTE-Cones-AdiabT_{1ρ} value was observed in cartilage with more extensive or full-thickness lesions based on WORMS score. The AUC values of UTE-Cones-AdiabT_{1ρ} for mild cartilage degeneration reached 0.8, with a diagnostic threshold value of 39.4 ms, a sensitivity of 80.8%, and a specificity of 63.5%. These preliminary results suggest the potential of UTE-Cones-AdiabT_{1ρ} as a promising biomarker for quantitative evaluation of early cartilage degeneration in OA patients.

The conventional T_{1ρ} imaging sequences have been extensively investigated for quantitative assessment of cartilage degeneration. Several ex vivo studies reported that T_{1ρ} relaxation time was sensitive to early biochemical changes, particularly PG depletion in articular cartilage (2–4). A number of clinical studies showed higher T_{1ρ} values in mild and moderate-severe OA (6–10). However, several other studies suggested that T_{1ρ} was associated with not only PG content, but water content, collagen content and collagen network integrity (40–41). T_{1ρ} mapping could not accurately measure cartilage PG content in human subjects with knee OA (41). The contradictory results might be partly due to the strong magic angle effect in conventional T_{1ρ} imaging (13–15).

The AdiabT_{1ρ} imaging sequence has attracted interest in recent years as an alternative to conventional T_{1ρ} imaging for quantitative assessment of cartilage degeneration, mostly due to its reduced sensitivity to both the magic angle effect and B1 inhomogeneity (27). The sensitivity of AdiabT_{1ρ} to cartilage degeneration has been further demonstrated by recent studies with animal models of OA (21–22), cadaveric human cartilage samples (23–24), as well as in vivo imaging (25–26).

Our results demonstrate that the 3D UTE-Cones-AdiabT_{1ρ} sequence could be used for high resolution imaging and quantitative assessment of knee cartilage degeneration at its early stages, with the observed trend of higher T_{1ρ} and AdiabT_{1ρ} values in more degenerated cartilage largely consistent across the literature (2–10, 21–26). Similar patterns have also been seen in subregional analysis (10). The correlation between UTE-Cones-AdiabT_{1ρ} and WORMS varied with the cartilage subregion: the central subregions of medial femoral cartilage and the posterior subregions of lateral femoral cartilage showed more profound UTE-Cones-AdiabT_{1ρ} increases with degeneration. Those same regions produced higher T_{1ρ} values in a study by Wang et al. (10). The anterior subregions of medial tibial cartilage, on the other hand, showed significant increases in UTE-Cones-AdiabT_{1ρ} values but not in T_{1ρ} values with cartilage degeneration based on WORMS scores. Furthermore, there was no significant difference in UTE-Cones-AdiabT_{1ρ} values between doubtful-minimal OA and moderate-severe OA, and there was no significant difference in the UTE-Cones-AdiabT_{1ρ} values among adjacent WORMS groups (e.g., WORMS=1 vs. WORMS=2; WORMS=2 vs. WORMS=2.5; WORMS=2.5 vs. WORMS=3; etc.).

The 3D UTE-Cones-AdiabT_{1ρ} sequence has several advantages over conventional morphological imaging as well as quantitative T₂ and T_{1ρ} sequences. First, the biomarker UTE-Cones-AdiabT_{1ρ} is relatively insensitive to the magic angle effect (30–32). In a prior study over eight patellae reoriented from parallel to near 54° relative to the B₀ field, the average Cones-AdiabT_{1ρ} value increased by 27%, much lower than the 77% increase observed in continuous wave T_{1ρ} and the 238% increase observed in T₂* (32). Similar results have been reported in several other studies (12–14). Second, the 3D UTE-Cones-AdiabT_{1ρ} sequence is highly time-efficient with reduced motion sensitivity (34). Data acquisition is based on a 3D spiral acquisition with conical view ordering; the k-space trajectory is more radial in the center of k-space for fast coverage of low spatial frequency data, and more curved in the outer k-space for higher sampling efficiency. The repeated sampling of the center of k-space provides quantitative AdiabT_{1ρ} imaging with reduced sensitivity to motion (29). Third, although we focused on OA's progressive loss of articular cartilage in this study, it is, in reality, a heterogeneous and multifactorial disease that involves all major knee joint tissues. Conventional sequences have difficulty imaging tissues or tissue components with short T₂ relaxation times, such as the deep cartilage, menisci, ligaments, and tendons, prohibiting a “whole-organ” approach to knee joint degeneration (17–20). The 3D UTE-Cones-AdiabT_{1ρ} sequence has the potential to overcome this major limitation associated with conventional T₂ and T_{1ρ} sequences.

There are several limitations of this study. First, the sample size was relatively small, with only 28 subjects for the doubtful-minimal OA group and 18 subjects for the moderate-severe OA group. A more systematic cross-sectional and especially longitudinal study with a larger

sample size is needed to increase the confidence in measuring changes associated with early OA. Second, there were no gold standard histological examinations available in this study. KL grade and WOMBS were used as the clinical evaluation criteria. However, it is well known that both KL grade and WOMBS have many limitations and cannot provide accurate assessment of cartilage degeneration, especially at its early stages. The relationship between UTE-Cones-AdiabT_{1ρ} values and histopathological changes in articular cartilage still needs to be investigated. Third, only UTE-Cones-AdiabT_{1ρ} was investigated in this study. No comprehensive comparisons were made with other quantitative UTE parameters such as T1, T_{1ρ}, Adiabatic T_{1ρ}, T2, T2*, magnetization transfer ratio, or macromolecular fraction. A biomarker panel approach involving all the aforementioned quantitative UTE biomarkers is likely to provide a more robust detection of OA. Fourth, only articular cartilage was analyzed in this study. Because the currently widely used grading system, WOMBS, is largely based on morphological imaging of the knee joint with a focus on the articular cartilage (33), a systematic evaluation of UTE-Cones-AdiabT_{1ρ} values for all the principal components in the knee joint, including the menisci, ligaments, tendons, muscles, and bones, was not conducted. There are no grading systems available which involve morphological and quantitative imaging of all major knee joint tissues, especially tissues with short T₂ relaxation times. Clearly, further research is needed in this area.

Conclusion

The UTE-Cones-AdiabT_{1ρ} biomarker can distinguish mild cartilage degeneration from normal cartilage, with a higher UTE-Cones-AdiabT_{1ρ} value for more degenerated cartilage. The 3D UTE-Cones-AdiabT_{1ρ} sequence may significantly improve the robustness in quantitative systematic evaluation of knee joint degeneration.

Acknowledgements:

The authors acknowledge grant support from NIH (R01AR062581, R01AR068987, R01AR075825, R01AR078877, and R21AR075851), the VA Clinical Science Research & Development Service (1101CX001388 and I21RX002367), and GE Healthcare.

Abbreviations

AdiabT_{1ρ}	adiabatic T _{1ρ}
AFI	actual flip angle
FA	flip angle
ICC	Intraclass correlation efficient
IRB	Institutional Review Board
KL	Kellgren-Lawrence
N_{IR}	number of inversion recovery
N_{sp}	number of spokes

OA	osteoarthritis
PG	proteoglycan
RF	radiofrequency
3D	Three-dimensional
TSLs	spin-locking times
T_{1ρ}	Spin lattice relaxation in the rotating frame
UTE	ultrashort echo time
VFA	variable flip angles
WORMS	Whole-Organ Magnetic-Resonance-Imaging Score

References

1. Redfield AG. Nuclear Magnetic Resonance Saturation and Rotary Saturation in Solids. *Phys Rev.* 1955; 98:1787–1809.
2. Duvvuri U, Reddy R, Patel SD, Kaufman JH, Kneeland JB, Leigh JS. T_{1ρ}-relaxation in articular cartilage: effects of enzymatic degradation. *Magn Reson Med.* 1997; 38:863–867. [PubMed: 9402184]
3. Akella SV, Regatte RR, Gougoutas AJ, et al. Proteoglycan-induced changes in T_{1ρ}-relaxation of articular cartilage at 4T. *Magn Reson Med.* 2001; 46:419–423. [PubMed: 11550230]
4. Regatte RR, Akella SV, Borthakur A, Reddy R. Proton spin-lock ratio imaging for quantitation of glycosaminoglycans in articular cartilage. *J Magn Reson Imaging.* 2003; 17:114–121. [PubMed: 12500280]
5. Keenan KE, Besier TF, Pauly JM, et al. Prediction of glycosaminoglycan content in human cartilage by age, T_{1ρ} and T₂ MRI. *Osteoarthritis Cartilage* 2011; 19:171–179. [PubMed: 21112409]
6. Regatte RR, Akella SVS, Wheaton AJ, et al. 3D-T_{1ρ}-relaxation mapping of articular cartilage: in vivo assessment of early degenerative changes in symptomatic osteoarthritic subjects. *Acad Radiol.* 2004; 11:741–749. [PubMed: 15217591]
7. Pakin SK, Xu J, Schweitzer ME, Regatte RR. Rapid 3D-T_{1ρ} mapping of the knee joint at 3.0T with parallel imaging. *Magn Reson Med.* 2006; 56:563–571. [PubMed: 16894582]
8. Blumenkrantz G, Majumdar S. Quantitative magnetic resonance imaging of articular cartilage in osteoarthritis. *Eur Cell Mater.* 2007; 13:76–86. [PubMed: 17506024]
9. Li X, Benjamin Ma C, Link TM, et al. In vivo T_{1ρ} and T₂ mapping of articular cartilage in osteoarthritis of the knee using 3T MRI. *Osteoarthr Cartilage.* 2007; 15:789–797.
10. Wang L, Chang G, Xu J, et al. T_{1ρ} MRI of menisci and cartilage in patients with osteoarthritis at 3T. *Eur J Radiol.* 2012; 81: 2329–2336. [PubMed: 21908122]
11. Mlynarik V, Szomolanyi P, Toffanin R, Vittur F, Trattnig S. Transverse relaxation mechanisms in articular cartilage. *J Magn Reson.* 2004; 169:300–307. [PubMed: 15261626]
12. Wang N, Xia Y. Dependencies of multi-component T₂ and T_{1ρ} relaxation on the anisotropy of collagen fibrils in bovine nasal cartilage. *J Magn Reson.* 2011; 212:124–132. [PubMed: 21788148]
13. Du J, Stantum S, Znamirovski R, Bydder GM, Chung CB. Ultrashort TE T_{1ρ} magic angle imaging. *Magn Reson Med.* 2013; 69:682–687. [PubMed: 22539354]
14. Shao H, Pauli C, Li S, et al. Magic angle effect plays a major role in both T_{1ρ} and T₂ relaxation in articular cartilage. *Osteoarthritis Cartilage.* 2017; 25:2022–2030. [PubMed: 28161394]
15. Roemer FW, Kijowski R, Guermazi A. Editorial: from theory to practice – the challenges of compositional MRI in osteoarthritis research. *Osteoarthritis Cartilage.* 2017; 25:1923–1925. [PubMed: 28844567]

16. Mosher TJ, Smith H, Dardzinski BJ, Schmithorst VJ, Smith MB. MR imaging and T2 mapping of femoral cartilage: in vivo determination of the magic angle effect. *AJR*. 2001; 177:665–669. [PubMed: 11517068]
17. Brandt KD, Radin EL, Dieppe PA, Putte L. Yet more evidence that osteoarthritis is not a cartilage disease (Editorial). *Ann Rheum Dis*. 2006; 65:1261–1264. [PubMed: 16973787]
18. Hunter DJ, Zhang YQ, Niu JB, et al. The association of meniscal pathologic changes with cartilage loss in symptomatic knee osteoarthritis. *Arthritis Rheum*. 2006; 54:795–801. [PubMed: 16508930]
19. Tan AL, Toumi H, Benjamin M, et al. Combined high-resolution magnetic resonance imaging and histological examination to explore the role of ligaments and tendons in the phenotypic expression of early hand osteoarthritis. *Ann Rheum Dis*. 2006; 65:1267–1272. [PubMed: 16627540]
20. Chang EY, Du J, Chung CB. UTE imaging in the musculoskeletal system. *J Magn Reson Imaging*. 2015; 41(4):870–883. [PubMed: 25045018]
21. Ellermann J, Ling W, Nissi MJ, et al. MRI rotating frame relaxation measurements for articular cartilage assessment. *Magn Reson Imaging*. 2013; 31(9):1537–1543. [PubMed: 23993794]
22. Rautiainen J, Nissi MJ, Liimatainen T, Herzog W, Korhonen RK, Nieminen MT. Adiabatic rotating frame relaxation of MRI reveals early cartilage degeneration in a rabbit model of anterior cruciate ligament transection. *Osteoarthritis and Cartilage*. 2014; 22:1444–1452. [PubMed: 25278055]
23. Nissi MJ, Salo EN, Tiitu V, et al. Multi-parametric MRI characterization of enzymatically degraded articular cartilage. *J Orthopaedic Research*. 2016; 34:1111–1120.
24. Rautiainen J, Nissi MJ, Salo E, et al. Multiparametric MRI assessment of human articular cartilage degeneration: correlation with quantitative histology and mechanical properties. *Magn Reson Med*. 2015; 74:249–259.
25. Casula V, Autio J, Nissi MJ, et al. Validation and optimization of adiabatic T1rho and T2rho for quantitative imaging of articular cartilage at 3T. *Magn Reson Med*. 2017; 77:1265–1275. [PubMed: 26946182]
26. Casula V, Nissi MJ, Podlipska J, et al. Elevated adiabatic T1rho and T2 in articular cartilage are associated with cartilage and bone lesions in early osteoarthritis: a preliminary study. *J Magn Reson Imaging*. 2017; 46:678–689. [PubMed: 28117922]
27. Hänninen N, Rautiainen J, Rieppo L, Saarakkala S, Nissi MJ. Orientation anisotropy of quantitative MRI relaxation parameters in ordered tissue. *Sci Rep*. 2017; 7:9606. [PubMed: 28852032]
28. Ma YJ, Carl M, Shao H, Tadros AS, Chang EY, Du J. Three-dimensional ultrashort echo time cones T1rho (3D UTE-cones-T1rho) imaging. *NMR Biomed*. 2017; 30:3709.
29. Wu M, Zhao W, Wan L, et al. Quantitative three-dimensional ultrashort echo time cones imaging of the knee joint with motion correction. *NMR in Biomedicine*. 2020; 33(1): e4214. [PubMed: 31713936]
30. Ma Y, Carl M, Searleman A, Lu X, Chang EY, Du J. Three dimensional adiabatic T1rho prepared ultrashort echo time Cones (3D AdiabT1rho UTE-Cones) sequence for whole knee imaging. *Magn Reson Med*. 2018; 80(4):1429–1439. [PubMed: 29493004]
31. Wu M, Ma Y, Wan L, et al. Magic angle effect on adiabatic T1rho imaging of the Achilles tendon using 3D ultrashort echo time cones trajectory. *NMR in Biomedicine*. 2020; 33(8): e4322. [PubMed: 32431025]
32. Wu M, Ma Y, Kasibhatla A, et al. Convincing Evidence for Magic Angle Less-Sensitive Quantitative T1rho Imaging of Articular Cartilage Using the 3D Ultrashort Echo Time Cones Adiabatic T1rho (3D UTE Cones-AdiabT1rho) Sequence. *Magn Reson Med*. 2020; 84(5): 2551–2560. [PubMed: 32419199]
33. Peterfy CG, Guermazi A, Zaim S, et al. Whole-Organ Magnetic Resonance Imaging Score (WORMS) of the knee in osteoarthritis. *Osteoarthritis Cartilage*. 2004; 12:177–190. [PubMed: 14972335]
34. Carl M, Bydder GM, Du J. UTE imaging with simultaneous water and fat signal suppression using a time-efficient multispoke inversion recovery pulse sequence. *Magn Reson Med*. 2016; 76:577–582. [PubMed: 26309221]
35. Garwood M, DelaBarre L. The return of the frequency sweep: designing adiabatic pulses for contemporary NMR. *J Magn Reson*. 2001; 153(2):155–177. [PubMed: 11740891]

36. Ma YJ, Zhao W, Wan L, et al. Whole knee joint T1 values measured in vivo at 3T by combined 3D ultrashort echo time cones actual flip angle and variable flip angle methods. *Magn Reson Med*. 2019; 81:1634–1644. [PubMed: 30443925]
37. Ma YJ, Lu X, Carl M, et al. Accurate T1 mapping of short T2 tissues using a three-dimensional ultrashort echo time cones actual flip angle – variable TR (3D UTE-Cones AFI-VTR) method. *Magn Reson Med*. 2018; 80:598–608. [PubMed: 29314235]
38. Klein S, Staring M, Murphy K, Viergever MA, Pluim JP. Elastix: A toolbox for intensity-based medical image registration. *IEEE Trans Med Imaging*. 2010; 29:196–205. [PubMed: 19923044]
39. Guermazi A, Eckstein F, Hayashi D, et al. Baseline radiographic osteoarthritis and semi-quantitatively assessed meniscal damage and extrusion and cartilage damage on MRI is related to quantitatively defined cartilage thickness loss in knee osteoarthritis: The Multicenter Osteoarthritis Study. *Osteoarthritis Cartilage*. 2015; 23:2191–2198. [PubMed: 26162806]
40. Thuring J, Linka K, Itskov M, et al. Multiparametric MRI and Computational Modelling in the Assessment of Human Articular Cartilage Properties: A Comprehensive Approach. *Biomed Res Int*. 2018; 9460456.
41. Van Tiel J, Kotek G, Reijman M, et al. Is T1rho Mapping an Alternative to Delayed Gadolinium-enhanced MR Imaging of Cartilage in the Assessment of Sulphated Glycosaminoglycan Content in Human Osteoarthritic Knees? An in Vivo Validation Study. *Radiology*. 2016; 279:523–531. [PubMed: 26588020]

Key points:

The 3D UTE-Cones-AdiabT_{1ρ} sequence can distinguish mild cartilage degeneration from normal cartilage with a diagnostic threshold value of 39.4 ms for mild cartilage degeneration with 80.8% sensitivity.

Higher UTE-Cones-AdiabT_{1ρ} values were observed in both larger and deeper lesions in the articular cartilage.

UTE-Cones-AdiabT_{1ρ} is a promising biomarker for quantitative evaluation of early cartilage degeneration.

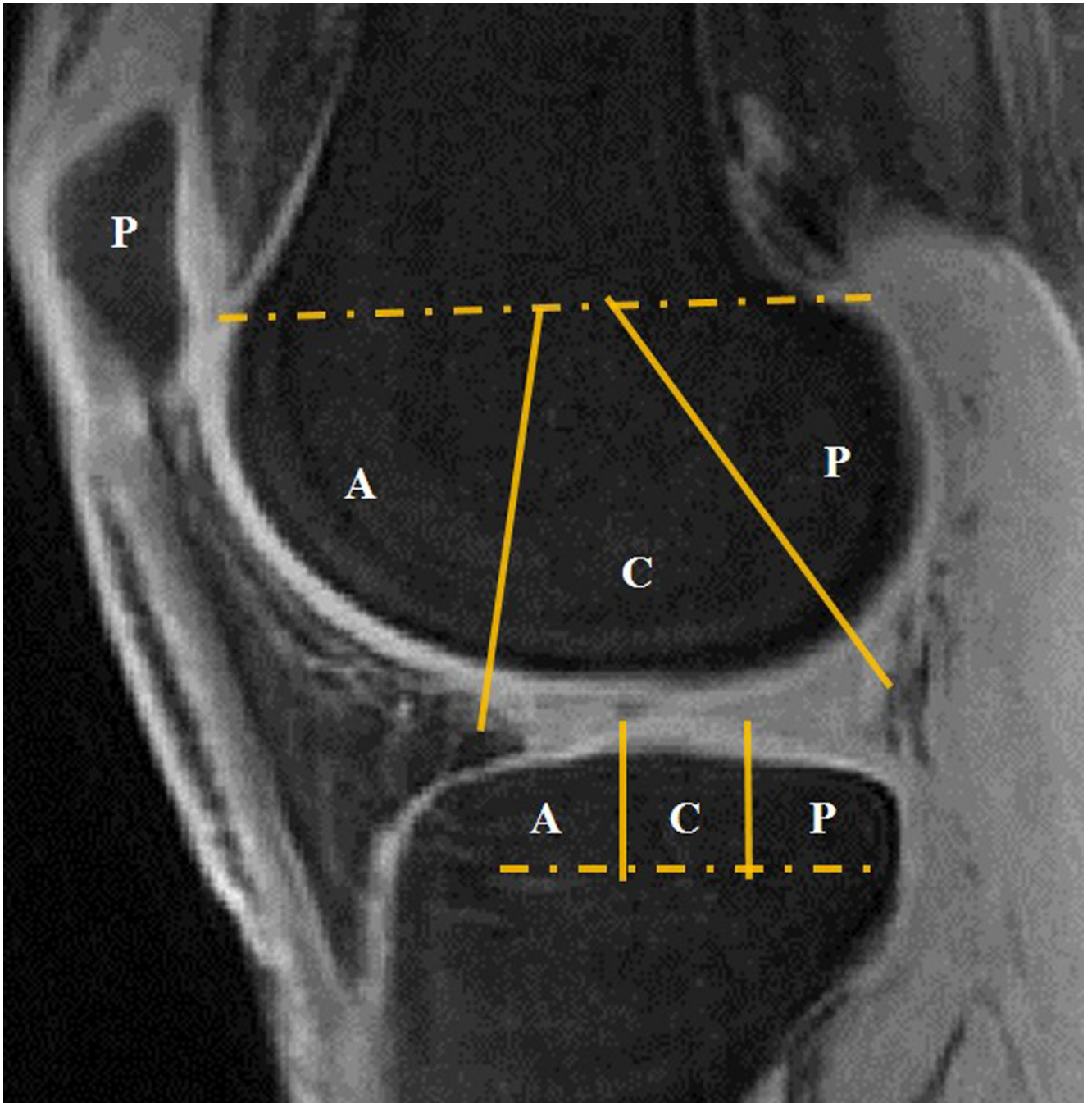


Figure 1.

Regional subdivision of the articular surfaces. The femoral and tibial condyles are divided into medial (M) and lateral (L) regions, with the trochlear groove of the femur considered part of the M region. Then the femoral and tibial surfaces are further subdivided into anterior (A), central (C) and posterior (P) regions. The tibial surface is divided into three regions equally. The femoral anterior surface (A): extending from the anterior-superior osteochondral junction to the anterior margin of the anterior horn of the meniscus; The femoral posterior surface (P): extending from the posterior capsular attachment of the

posterior horn of the meniscus to the posterior-superior osteochondral junction. The patella works as a whole.

Author Manuscript

Author Manuscript

Author Manuscript

Author Manuscript

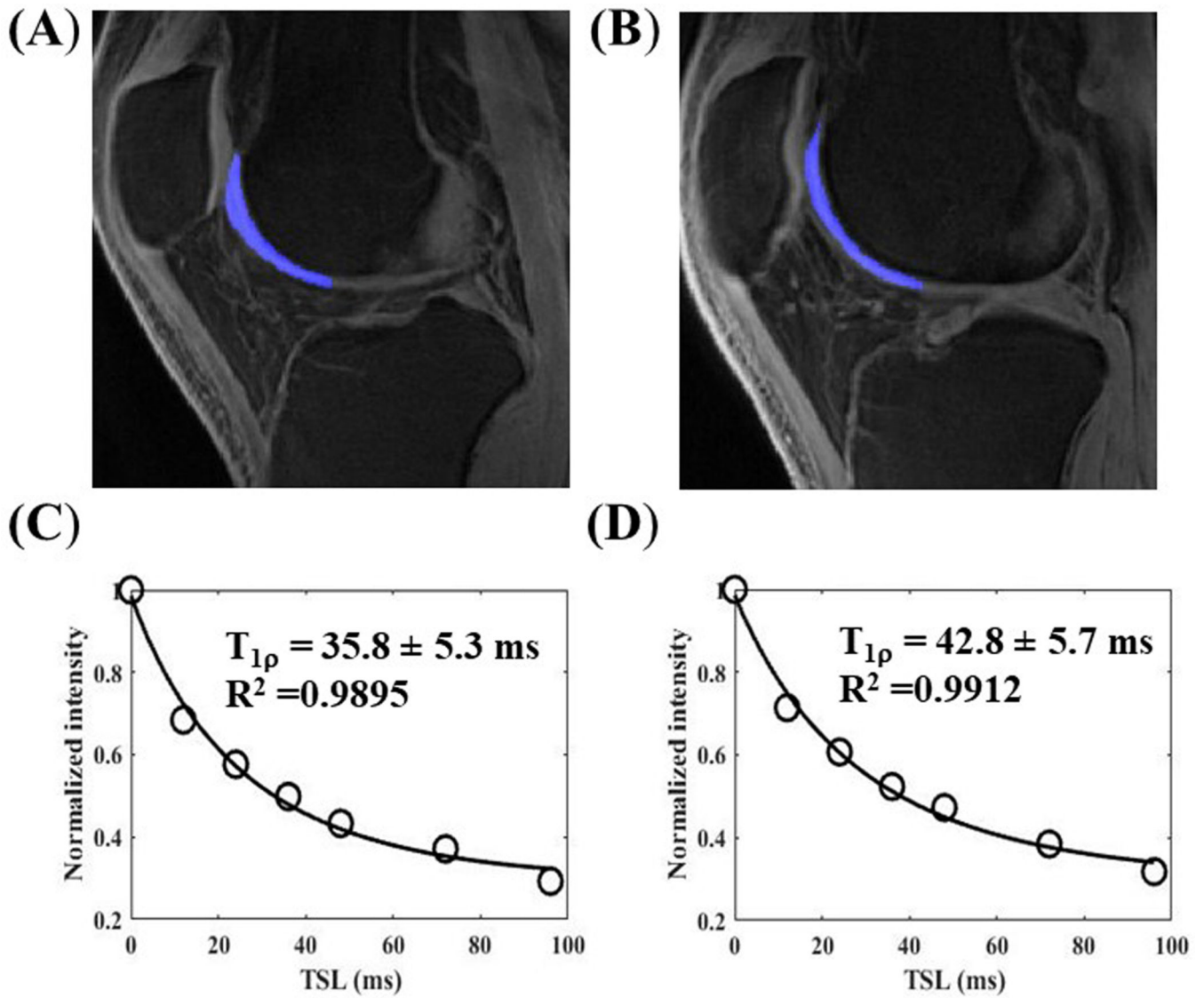


Figure 2. Excellent single-component exponential $T_{1\rho}$ fitting was achieved for normal cartilage (A, C) ($T_{1\rho}=35.8\pm 5.3$ ms) in a 36 years old healthy volunteer and abnormal cartilage (B, D) (WORMS=2, $T_{1\rho}=42.8\pm 5.7$ ms) in a 43 years old patient with doubtful-minimal OA.

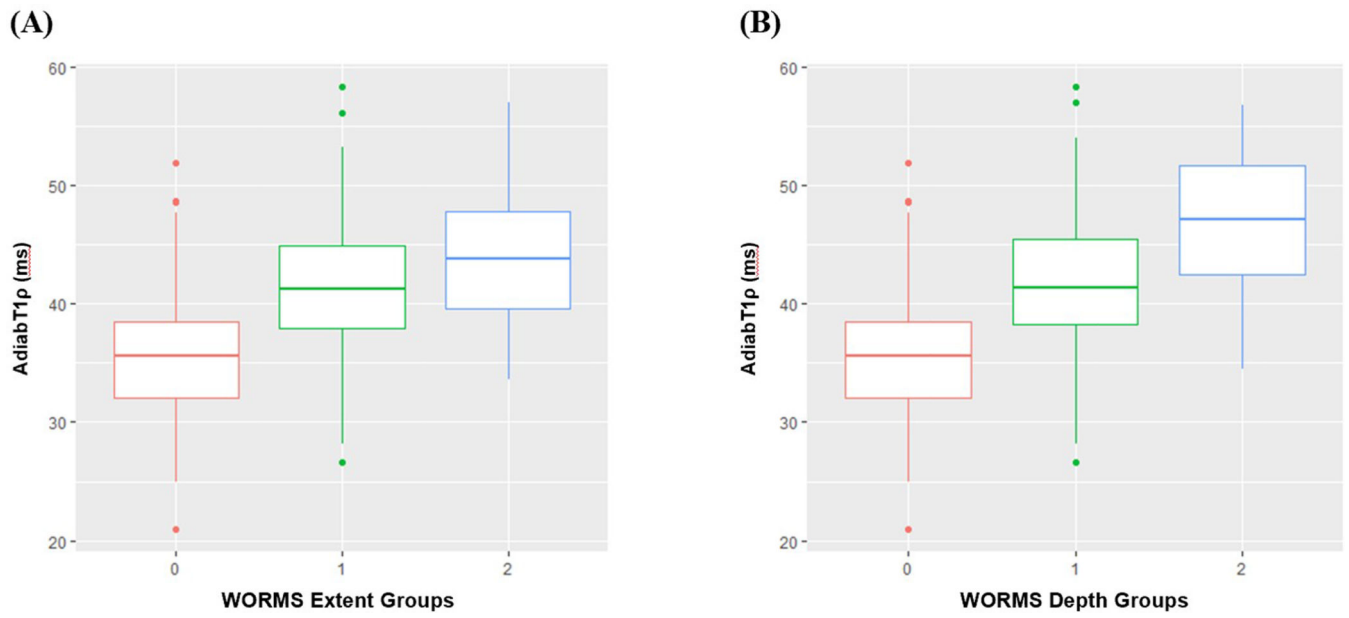


Figure 3. Boxplot of UTE-Cones-AdiabT1ρ values in different WORMS extent groups (A) and WORMS depth groups (B).

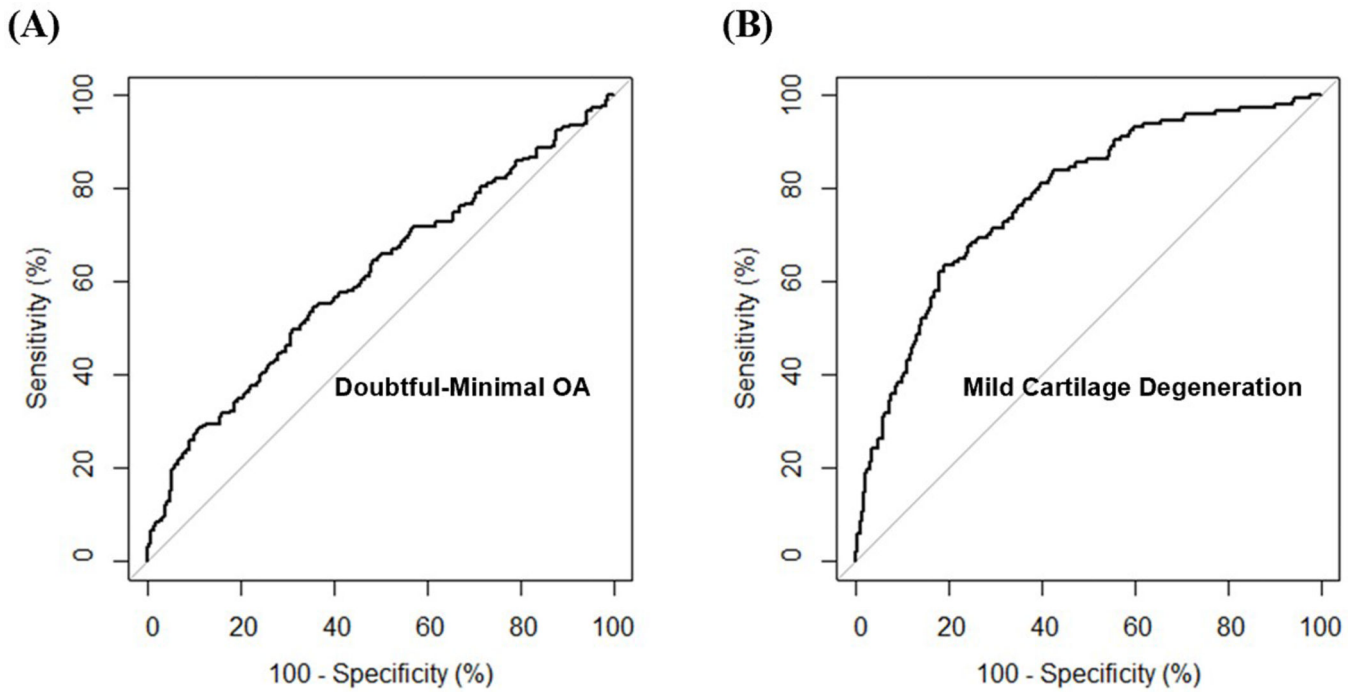


Figure 4.

(A) and (B) show ROC curves of AdiabT_{1ρ} for the diagnosis of doubtful-minimal OA (KL=1–2) and mild cartilage degeneration (WORMS=1). The AUCs of AdiabT_{1ρ} for doubtful-minimal OA and mild cartilage degeneration are 0.6 and 0.8. The corresponding cutoff points are AdiabT_{1ρ} 38.5 ms for doubtful-minimal OA and AdiabT_{1ρ} 39.4 ms for mild cartilage degeneration.

Table 1.

The grouping of subjects and subregion cartilages according to KL grade and WORMS.

KL grouping		Normal controls		Doubtful-minimal OA		Moderate-severe OA	
KL grade		0		1–2		3–4	
Subjects		20 (30.3%)		28 (42.4%)		18 (27.3%)	
WORMS grouping	0	1	2	2.5	3	4	5
Subregion cartilages	391 (54.8%)	148 (20.8%)	65 (9.1%)	6 (0.8%)	71 (10%)	5 (0.7%)	27 (3.8%)
Extent groups		Normal cartilage		Regional lesions		Diffuse lesions	
WORMS		0		1, 2, 2.5		3, 4, 5	
Subregion cartilages		391 (54.8%)		219 (30.7%)		103 (14.4%)	
Depth groups		Normal cartilage		Partial-thickness lesions		Full-thickness lesions	
WORMS		0		1, 2, 2.5		3, 4, 5	
Subregion cartilages		391 (54.8%)		289 (40.5%)		33 (4.6%)	

Table 2.Mean UTE-Cones-AdiabT_{1ρ} (ms) in different WORMS groups

WORMS	0	1	2	2.5	3	4	5
AdiabT _{1ρ}	35.5±5.0	40.8±5.0	42.8±5.3	45.3±6.6	43.1±5.1	43.9±5.2	47.7±5.8
Extent groups	Normal cartilage (WORMS 0)		Regional lesions (WORMS 1,2,2.5)		Diffuse lesions (WORMS 3,4,5)		
AdiabT _{1ρ}	35.5±5.0		41.5±5.3		44.1±5.6		
Depth groups	Normal cartilage (WORMS 0)		Partial-thickness lesions (WORMS 1,2,3,4)		Full-thickness lesions (WORMS 2.5,5)		
AdiabT _{1ρ}	35.5±5.0		41.8±5.2		46.8±6.5		

Author Manuscript

Author Manuscript

Author Manuscript

Author Manuscript

Table 3

UTE-Cones-AdiabT_{1ρ} values (mean ± SD) and 95% confidence intervals (CI) in different subregions and Spearman's correlation between UTE-Cones-AdiabT_{1ρ} and WORMS.

Subregions	N	AdiabT _{1ρ} (ms)	95%CI	Relationship between AdiabT _{1ρ} and WORMS	
MFa	60	39.8 ± 4.5	38.7 to 41.0	r = 0.39	P<0.05
LFa	59	39.0 ± 3.9	38.0 to 40.0	r = 0.35	P<0.05
MFc	48	41.1 ± 5.0	39.6 to 42.5	r = 0.74	P<0.05
LFc	57	41.8 ± 3.9	40.8 to 42.8	r = 0.39	P<0.05
MFp	51	43.2 ± 5.6	41.6 to 44.7	r = 0.57	P<0.05
LFp	56	41.5 ± 5.9	39.9 to 43.1	r = 0.75	P<0.05
MF	159	41.3 ± 5.2	40.5 to 42.1	r = 0.42	P<0.05
LF	172	40.8 ± 4.8	40.0 to 41.5	r = 0.43	P<0.05
F	331	41.0 ± 5.0	40.5 to 41.5	r = 0.42	P<0.05
P	58	45.8 ± 5.0	44.5 to 47.1	r = 0.43	P<0.05
MTa	51	34.2 ± 4.7	32.8 to 35.5	r = 0.61	P<0.05
LTa	56	35.3 ± 4.9	34.0 to 36.7	r = 0.54	P<0.05
MTc	53	32.9 ± 4.6	31.6 to 34.2	r = 0.49	P<0.05
LTc	56	35.1 ± 4.9	33.8 to 36.4	r = 0.53	P<0.05
MTp	53	33.5 ± 5.5	32.0 to 35.0	r = 0.52	P<0.05
LTp	55	37.8 ± 4.2	36.7 to 38.9	r = 0.28	P<0.05
MT	157	33.5 ± 4.9	32.7 to 34.3	r = 0.55	P<0.05
LT	167	36.1 ± 4.8	35.3 to 36.8	r = 0.46	P<0.05
T	324	34.8 ± 5.0	34.3 to 35.4	r = 0.54	P<0.05

Note: M = medial, L = lateral, F = femoral condyle, T = tibial plateau, P = patella, a = anterior, c = central, p = posterior.